Acta Neurochirurgica (2024) 166:470
https://doi.org/10.1007/s00701-024-06361-y

RESEARCH

Early osteointegration in "one-step" resection and reconstruction using porous hydroxyapatite custom implants for skull-infiltrating tumors: a monocentric prospective series

Raffaella Messina[1] · Luca Speranzon[1] · Luigi de Gennaro[1] · Enrico Maria Nigri[1] · Mariagrazia Dibenedetto[1] · Maria Teresa Bozzi[1] · Carlo Delvecchio[1] · Francesco Signorelli[1]

Received: 23 August 2024 / Accepted: 11 November 2024

Abstract

Background Early reconstruction of the skull represents the gold standard after resection of bone infiltrating cranial tumors. Customized hydroxyapatite porous ceramics are an excellent option for covering skull bone defects. The authors illustrate the surgical technique and investigate the effectiveness of the "one-step" procedure in terms of aesthetic results and early degree of osteointegration.

Method A prospective study was conducted, including all patients operated on for skull bone infiltrating lesions at our center between January 2020 and June 2022. Stereolithography was the technique used for shaping the epoxy-resin model, suitable for both designing the craniotomy and manufacturing the custom-made hydroxyapatite prosthesis. Clinical outcome, results of early (6-week) and late (3-month) osteointegration evaluated on CT and MRI, and level of patient satisfaction measured by the FACE-Q questionnaire were reported.

Results Fourteen patients (13 adults and a 7-year-old boy) and a total of 15 implants were included. The average percentage of early osteointegration calculated at the edge of the prosthesis, was 72.2%, that increased to 82.6% after 3 months. Patient-reported outcomes indicated a high level of satisfaction across all patients.

Conclusions "One-step" resection and reconstruction using customized hydroxyapatite porous implants for treatment of skull infiltrating tumors is a safe, simple and effective technique, in particular when the bone defect is large. Bone regeneration around and inside the prosthesis seems to start early after surgery.

Keywords "One-Step" procedure · Skull bone tumors · Bone reconstructive surgery · Custom-made implant

Introduction

Reconstructing bone integrity after tumor resection in the calvaria or skull base is essential for both functional and aesthetic purposes. Common cranioplasty materials include metals like titanium, polymers such as polyetheretherketone (PEEK) or polymethyilmethacrylate (PMMA), and ceramics like hydroxyapatite (HA) [5, 25]. Previous studies have evaluated the complications and outcomes associated with these materials, including their use following decompressive craniectomy [18]. Significant advancements have been made to enhance the biocompatibility, strength, sterilization, and

✉ Raffaella Messina
raffamessina@gmail.com

Luca Speranzon
drsperanzon@gmail.com

Luigi de Gennaro
luigidegen95@gmail.com

Enrico Maria Nigri
enrico.nigri01@gmail.com

Mariagrazia Dibenedetto
dibenedettomariagrazia@gmail.com

Maria Teresa Bozzi
mari-ta@hotmail.it

Carlo Delvecchio
carlo.delvecchio@policlinico.ba.it

Francesco Signorelli
francesco.signorelli@uniba.it

[1] Division of Neurosurgery, Department of Translational Biomedicine and Neurosciences (DiBraiN), University of Bari "Aldo Moro", University Hospital Policlinico of Bari, Bari, Italy

Published online: 22 November 2024

design simplicity of cranioplasty materials. While no material has emerged as universally superior, the choice often depends on the type of surgery and patient-specific needs [23, 30]. HA stands out for its biocompatibility and osteoconductive properties, mimicking natural bone, which leads to improved bone anchorage, a lower risk of foreign body reactions, fewer implant revisions, and enhanced aesthetic outcomes [1, 2, 15, 44, 46, 50].

Traditionally, bone reconstruction after tumor resection required a two-step process: tumor removal followed by reconstructive surgery [4, 8, 9, 11, 20, 53]. Recent advancements, however, have enabled both procedures to be performed in a single session using custom-made implants [12]. Laser lithographic molding techniques allow for patient-specific cranioplasty designs based on CT data. Over the past decade, the "one-step" technique for tumor resection and simultaneous reconstruction has gained attention, offering advantages such as reduced infection risk, minimized manual manipulation, and better aesthetic and functional outcomes [4, 13, 36, 37]. Though many studies have focused on alloplastic materials, only a few have examined the use of HA in this context. The "one-step" approach has shown particular promise in managing large cranial tumors [33, 45, 47], preventing complications like iatrogenic craniolacunia and "sinking skin flap" syndrome, which can negatively affect cerebral glucose metabolism and intracranial pressure dynamics [52].

Despite advancements in cranioplasty techniques, limited data are available on the osteointegration timing of HA implants. While previous studies suggest that osteointegration is usually completed within two years [7, 22, 32, 42], the precise onset remains uncertain. To address this gap, our study aimed to assess early osteointegration rates in patients, using CT scans to evaluate bone density and MRI to detect fibrovascular tissue formation at the bone-prosthesis interface. Our interest in evaluating the clinical benefits of HA, combined with a focus on aesthetic quality and implant stability, led us to conduct this research.

This study presents our findings on early osteointegration and aesthetic outcomes using the "one-step" resection and reconstruction technique in patients who underwent custom-made porous HA cranioplasty for large cranial tumors.

Methods and materials

All patients treated in our center between January 2020 and June 2022 and undergoing a craniotomy for cranial bone infiltrating tumors, were analyzed. In order to make the sample representative for the purpose of the study, the population was screened based on the following inclusion and exclusion criteria:

1. Only patients who were candidates for single-step resection and reconstruction surgery, were included.
2. Among these, only patients who received a customized HA prosthesis, have entered the final sample.
3. Decompressive craniectomy-related clinical cases were not included.
4. Patients who had previously been treated with other alloplastic materials were not included.

Demographic, clinical, radiological data by CT and, when available, by MRI imaging and histology were recorded. Patients who did not have clinical and radiological follow-up data for at least 2 years after surgery were not included in the study.

Outcome assessment

Outcomes were assessed based on three criteria:

1. **Early and late osteointegration and bone regeneration rate**: evaluated using 6-week and 3-month postoperative head CT scans and MRI when available.
2. **Clinical results**: measured by the incidence of postoperative complications, including prosthesis fractures or dislocation.
3. **Aesthetic results**: assessed by comparing the symmetry of the treated side with the contralateral side, as evaluated by a radiologist, and by the patient's satisfaction using FACE-Q questionnaires (appearance, facial function, health-related quality of life, adverse effects) [26–28].

Radiological analysis and measure of osteointegration

Although CT images can be evaluated qualitatively to obtain an estimated percentage of the contour at which osteointegration has occurred, in accordance with the definition of osteointegration suggested by Staffa et al. [45], the quantitative analysis of osteointegration in our study was performed using Mimics software (Mimics Innovation Suite, Materialise, Leuven, Belgium) to quantify the percentage of the prosthesis contour where bony anchorage has occurred. This software processes 3D medical images from CT scans and MRIs, using the average Hounsfield Unit (HU) density of human bone as a reference, ranging from 400–700 HU for spongy bone to 1800–2000 HU for cortical bone [54]. The technique is based on measuring the Hounsfield units in every voxel at the bone-prosthesis interface, to calculate the total volume of the contact area. Then, a prearranged segmentation filter is applied to calculate the volume of

the contact area where osseous bridging has occurred [32], indicating osteointegration at the bone/implant margin. Following literature-reported methodologies [15, 32, 43], we used a segmentation filter of 400 HU in our sample as the threshold indicating the presence of osseous bridging. Thus, the osteointegration was measured by dividing the volume of the interface with HU > 400 by the total contact area. The percentage of osteointegration was calculated by examining four randomly but consistently chosen regions of interest (ROIs) along the prosthesis edge, using early postoperative head CT scans processed using MATLAB® software (The MathWorks Inc. 2022, MATLAB version: 9.13.0 (R2022b), Natick, Massachusetts https://www.mathworks.com) (Fig. 1A, B). Each ROI was graphically represented by a straight arrow along a 1 cm path, extending from 5 mm inside the host bone to 5 mm inside the prosthesis (Fig. 1C). The obtained HU histograms provided a density profile along that 1 cm path through each ROI. Data were then extrapolated from the central 2 mm of each arrow (straddling the bone/implant margin, 1 mm into the host bone and 1 mm into the implant), to calculate the percentage of osteointegration.

The concepts of bone regeneration and implant stability were indirectly estimated by measuring bone density in three nearly equal surface areas (two peripheral and one central) randomly selected by MATLAB® within the prosthesis (Fig. 1D), to observe the porous properties of hydroxyapatite, as demonstrated in previously published studies [10, 12, 14, 33, 44, 45].

The presence of fibrovascular tissue within the prosthesis pores, evident in postoperative T1-weighted gadolinium-enhanced MRI, was considered an additional indicator of HA implant integration with surrounding bone when available, as previously described [17, 32].

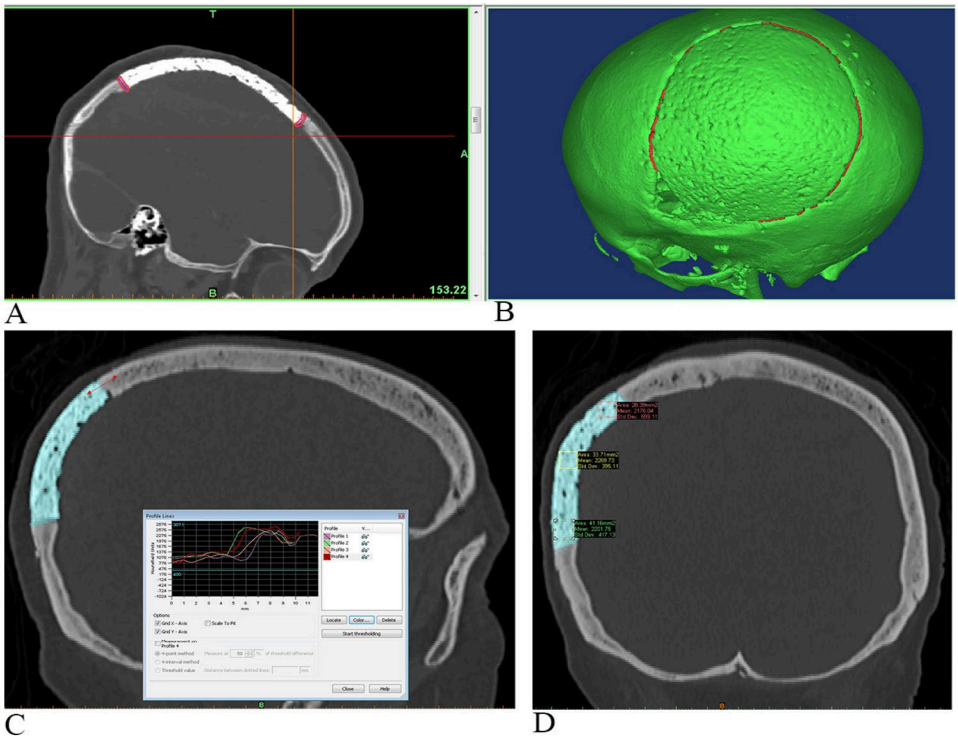

Fig. 1 Implant nº 13: **a** The area considered for the osteointegration analysis, 2 mm thick along the prosthesis edge, extending from 1 mm outside to 1 mm inside the prosthesis, is highlighted in red. **b** Implant nº. 13: the red line at the interface between the prosthesis and the host bone indicates their points of contact. **c** Implant nº 1: HU histogram consisting of four straight arrows 1 cm long, going from 5 mm inside the host bone to 5 mm inside the prosthesis, that represent four bone density profiles, randomly selected for each implant. The bone density profiles show that the custom-bone has a higher density than the one of natural bone. **d** Implant nº 1: the bone density was also evaluated into three areas of nearly equal surface (two peripheral areas and one central, indicated by the dashed squares) randomly selected by MATLAB® in the thickness of the prosthesis and expressed by mean HU density value and standard deviation

Custom bone service™ cranial prosthesis manufacturing

A customized 3D digital model of each patient's skull was created using thin-slice multiplanar CT scans (slice thickness ≈ 1 mm, Gantry tilt 0°) overlaid with preoperative MRI data for neuronavigation. While CT scans provided precise details of bone infiltration by the tumor, the extraosseous tumoral component was better visualized by MRI. The surgeon outlined the craniotomy borders based on the extent of bone invasion and desired resection margins on the 3D model. A virtual model of the prosthesis was then created and reviewed by the surgeon, who could modify or validate it, based on the desired extent of the craniotomy and shape of the symmetrical region of the skull of the patient. Adjustments to the prosthesis thickness and placement of suture holes for prosthesis anchorage were also possible at this stage. After approval, an epoxy resin 3D mold of the patient's skull, including the detachable cranioplasty component, was fabricated using 3D stereolithography. The final customized HA prosthesis (Fin-Ceramica Faenza, Italy) was then manufactured to replicate the 3D mold, with micropores (diameter < 10 µm) and macropores (diameter > 150 µm) resembling the mineral and structural composition of human bone.

Surgical procedure

A CT scan of the epoxy resin 3D model without the cranioplasty was merged with the patient's preoperative CT scan using StealthMerge software (Medtronic Italia SpA StealthStation™ Surgical Navigation System). Intraoperatively the patient's head was co-registered with the preoperative CT and MRI scans using face contours, and accuracy was confirmed by anatomical landmarks (e.g. tragus, canthus, nasion, nose tip, external acoustic meatus). The craniotomy margins were demarcated using the borders of the epoxy resin 3D model on both 2D and 3D neuronavigation views. The precise alignment of the prosthesis over the bony defect depended on this step. All "one-step" procedures were conducted using the Medtronic StealthStation S8 Navigation System.

Piezosurgery®. The "one-step" technique incorporated the use of a piezoelectric scalpel (Mectron SpA Cerasco, Italy) during the craniotomy step. This instrument facilitated precise bone cutting, minimized the bone gap, and maximized contact between the host bone and the prosthesis. It also allowed for adaptations of the HA prosthesis to the bony defect with minimal risk of damage. The prosthesis was anchored using not-absorbable synthetic sutures.

Before implantation, the prosthesis was soaked for 20 min in rifampicin (100 mg/ 100 ml saline solution). The total rifampicin dose depended on the prosthesis size, calculated by the volume of saline needed to fully submerge the prosthesis in a bowl. All implants in this series were associated with synthetic duraplasty (Neuro-Patch® B Braun and DuraGen® Integra) due to the infiltrative nature of the resected tumor, except for implants n°. 3 and 4.

Another technical consideration we addressed was the design of skin incision and the cutaneous flap. Vascular ingrowth and preservation of the dura mater were prioritized as the main goals guiding the incision choice [33, 40]. In each patient, the lesion's perimeter was exposed to ensure the reconstruction implant's margins aligned precisely within the craniotomy boundaries, as determined during presurgical planning. Our technical approach aimed to avoid the prosthesis overhanging the surrounding host bone or, conversely, being smaller than the craniotomy. The choice of skin incision was also influenced by the lesion's size and location of the lesion, allowing for a customized incision design for each patient. The skin flap design ensured that the suture line did not pass directly over the prosthesis-bone interface or the implant's fixation device.

FACE-Q conceptual framework

The aesthetic outcome and patient satisfaction with the procedure were assessed using the FACE-Q conceptual framework [26–28], a system for evaluating outcomes, satisfaction levels, and quality of life (QoL) in patients undergoing craniofacial surgery, aesthetic medicine procedures, and similar interventions with psychometric measures. Several FACE-Q questionnaire modules are available, each tailored to specific procedures or conditions (such as aesthetics, dental, paralysis, skin cancer, head and neck cancer, and pediatric head and neck cancer). In our study, a specific FACE-Q module for craniofacial surgery (Q-Portfolio© Techna Institute) was utilized [31]. The chosen module consists of four major sections (appearance, facial function, health-related quality of life, adverse effects), evaluating various aspects with scales and checklists. The FACE-Q assessment was conducted through sequential evaluations at each follow-up, using standardized patient photographs. At the end of follow-up, overall satisfaction was rated on a scale of 1 to 10 to assess the final outcome.

Results

Our study included 14 patients (5 males and 9 females), aged between 7 and 73 years (mean age 54.5 ± 17.1 SD). All patients had skull-infiltrating tumors affecting either

the calvaria or the skull-base. Each patient received a customized HA prosthesis using the "one step" procedure. In total, 15 implants were analyzed, as one patient required two subsequent implants (implant n° 9 and 10). Our cohort included patients with primary and metastatic bone-infiltrating neoplasms. The diagnosis ranged from meningioma of various histological grades (7 grade 1 meningiomas, 2 en-plaque atypical meningiomas, and one papillary grade 3 meningioma), to one case of fibrous dysplasia, one case of intradiploic cavernous hemangioma, to metastases from Ewing sarcoma and breast cancer. Demographic, radiological, clinical and histological characteristics of the cohort are detailed in Table 1. All 14 patients completed the postoperative follow-up. Regarding the postoperative complications, none of the implants had to be removed due to the typical complications of cranioplasty [18, 23, 30] (e.g., wound infection, subgaleal or intracranial empyema, pyogenic osteomyelitis; implant mobility or extrusion), and no cases of postoperative intracranial hemorrhage were reported. Two patients experienced wound dehiscence due to a CSF leak, respectively 7 days and 11 months postoperatively, the latter attributed to a recurrent WHO grade 3 meningioma. This patient underwent a second surgery for tumor recurrence, which required removal of the first implant (number 9) and placement of a second cranioplasty (number 10), designing a rotational scalp flap transfer. The oldest patient in our series developed bilateral subdural collections one-month post-procedure, which were treated conservatively, likely exacerbated by pre-existing brain atrophy. Another patient developed a persistent pseudomeningocele without CSF leak, which was managed with a subgaleal-peritoneal shunt two months after surgery. At an average follow-up of 6 months, no signs of prosthesis rejection, allergic reactions, fractures, or dislocations were reported. However, three patients passed away 10, 12, and 18- month post-surgery, due to treatment-resistant Ewing sarcoma, metastatic breast cancer, and a heart attack, respectively.

Table 2 presents the osteointegration data from 15 implants for 14 patients, based on Hounsfield analysis. The measurements were calculated using Mimics software on 6-week follow-up CT scans for all 13 adult patients and 20-week follow-up CT scans for the pediatric patient, scheduled later to minimize radiation exposure risks. All patients, underwent also a 3-month follow-up CT scan. The average

Table 1 Patient population: demographic, radiological and histological characteristics

Implant No	Gender	Age at surgery (years)	Side, Location	Symptoms and signs	Histology
1	F	58	R parietal osteolysis	Incidental	Brest-cancer metastasis
2	M	59	L fronto-parietal hyperostosis	Headache, L fronto-parietal swelling	En plaque atypical meningioma (grade 2)
3	F	49	R parietal transosseous lesion	R parietal swelling	Intradiploic cavernous hemangioma
4	M	34	L fronto-orbital «ground glass» lesion	Headache, L fronto-orbital swelling	Fibrous dysplasia
5	M	66	L fronto-parietal hyperostosis	Painful, L fronto-orbital swelling	Meningioma (grade 1)
6	F	63	L frontal –R parietal hyperostosis	R hemiparesis; dysarthria	Meningioma (grade 1)
7	M	73	R parietal hyperostosis	Ideomotor slowdown, L upper limb monoparesis	Meningioma (grade 1)
8	F	71	L fronto-sphenoidal hyperostosis	L eye decreased vision	En plaque atypical meningioma (grade 2)
9 (1st implant) 10 (2nd implant)	F	42	L fronto-parietal hyperostosis	R upper limb monoparesis	Papillary meningioma (grade 3)
11	F	66	R spheno-orbital hyperostosis	Headache, dizziness, R hypoacusia, R VI cranial nerve palsy	Meningioma (grade 1)
12	F	56	R temporal hyperostosis	Headache, R temporal swelling	Meningioma (grade 1)
13	M	7	L parietal transosseous lesion	Headache, L parietal swelling	Ewing sarcoma metastasis
14	F	64	L frontal hyperostosis	Incidental	Meningioma (grade 1)
15	F	55	L fronto-orbital hyperostosis	L eye proptosis, diplopia	Meningioma (grade 1)
Average		*54.5 years ± 17.1 SD*			

Table 2 Radiological results: CT and MRI analysis of osteointegration level

Implant	CT follow-up	Osteointegration percentage at host bone-implant margin
No	(weeks)	(filter 400 HU)
1	6	100%
2	6	93%
3	6	100%
4	6	96%
5	6	94%
6	6	78%
7	6	66%
8	6	91%
9	6 after 1st surgery	51% after 1st surgery
10	6 after 2nd look	26% after 2nd look
11	6	46%
12	6	11%
13	20	50%
14	6	88%
15	6	93%
Average	*6.9 weeks*	*72.2%*

osteointegration rate was 72.2% of normal bone density threshold on the early follow-up CT scan. This percentage was lowered by the inclusion of implants number 9 to 13, which displayed a gap between the prosthesis and the healthy bone due to the intraoperative decision to widen the bone removal area, prompted by unexpected tumor infiltration not evident in preoperative imaging. Notably, bone density measurement across the ROIs in our sample revealed an increasing gradient from host bone to implant. Our data also showed uniform density across the entire implant. Additionally, postoperative MRI osteointegration data were available for 6 out of 15 implants. For the remaining patients, postoperative MRI data were not available at the time of analysis. Positive contrast enhancement at the prosthesis-host bone interface was clearly observed in implant number 3 (which had 100% osteointegration) and was weaker in implants number 9 to 13 (with osteointegration percentages of 50% or less). At the 3-month CT scan, the average osteointegration rate was increased to 82.6%, confirming the uniform bone density across the implant in all cases.

All patients exhibited a symmetry between the treated and contralateral areas one month after surgery, following the resolution of postoperative soft tissue edema (Fig. 2). Patient-reported outcomes, as measured by the FACE-Q questionnaire, indicated a high level of satisfaction across all patients. Specifically, within the FACE-Q conceptual framework, which includes themes such as Satisfaction with Facial Appearance, Negative Sequelae, Satisfaction with Care, Health-related Quality of Life, the average overall general satisfaction index was 7.25 on a 10-point scale. This assessment was based on standardized photographs taken at each visit.

Discussion

This study provides valuable insights into the surgical management of large calvarial tumors, particularly through the use of custom-contoured alloplasts, with a focus on HA as

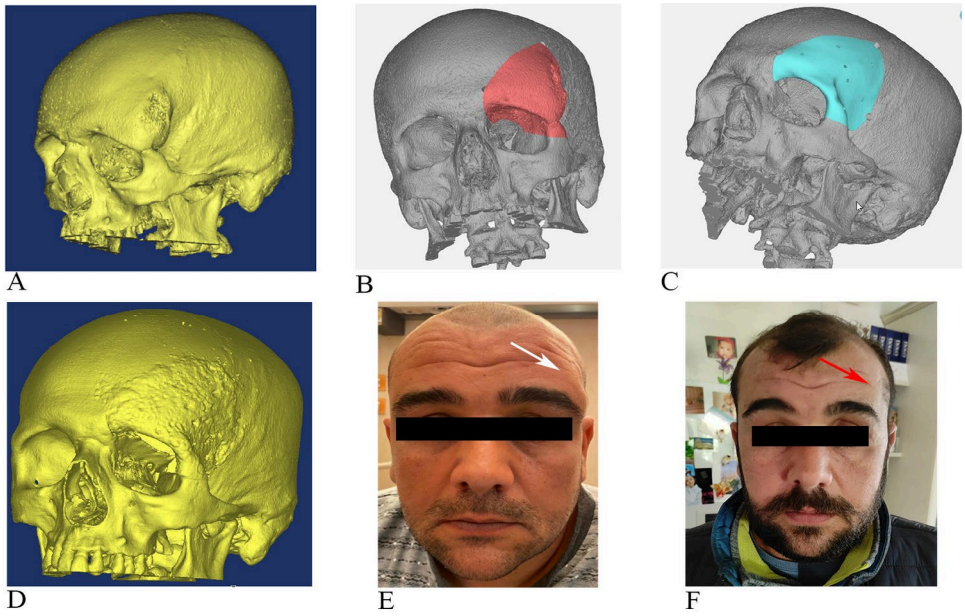

Fig. 2 Implant n° 4: **a** 3D preoperative CT scan with evidence of a left fronto-pterional-orbito-zygomatic osseous lesion (fibrous dysplasia). **b** and **c** 3D reconstruction respectively of the bone to be removed and of the 3D designed implant. **d** 3D 2-month postoperative CT scan showing the osteointegration of the cranioplasty. **e** and **f** Preoperative (**e**) and postoperative (**f**) patient's pictures, showing the preoperative skull deformity (**white arrow**) and the postoperative symmetry between the treated area and the controlateral one (**red arrow**)

the material of choice for cranioplasty. The results demonstrate that HA, when combined with advanced surgical tools like piezosurgery and neuronavigation, offers an effective and precise method for bone reconstruction. These findings are especially significant in enhancing osteointegration outcomes and improving patient satisfaction. A key novel finding of this study is the early onset of osteointegration, as evidenced by Hounsfield analysis on 6-week CT scans in adult patients and on 20-week CT scan for the child (Fig. 3). This early osteointegration suggests that HA's properties are conducive to rapid and effective integration with the host bone. This finding is critical as it indicates that the healing process begins soon after implantation, which is likely to contribute to the long-term success of the cranioplasty. The early healing process also contributes to reducing the risk of complications such as infections, which typically appear within the first month following surgery [51]. An earlier comparative study by Rubeli et al. evaluated the impact of standardized surveillance and an infection prevention bundle on surgical site infection rate after cranial neurosurgery [39]. The infection prevention bundle, in that study included standardized patient preparation, perioperative antibiotic/antiseptic use, barrier precautions, surgeon coaching, and the implementation of a specialized technical operation assistant team, all items included in a check-list, and was associated with a 53% reduced infection rate [39]. Our study's results, in addition to those recommendations already mentioned in the literature, suggest that the accuracy of the surgical technique, together with the single-step surgery and the use of porous HA as implant material, can accelerate the healing process and reduce the complications rates reported in literature for large cranial infiltrating tumors requiring scalp and/or skull reconstruction [35]. The healing process of our study cohort is also influenced by the notable pace of osteointegration, underscored by the progressive increase in bone density from early postoperative stages to the 3-month follow-up. Specifically, the average osteointegration rate at the 6-week follow-up CT scan was 72.2% of the normal bone density threshold, but even more compelling is the significant increase in the osteointegration rate to 82.6% by the 3-month CT scan. This 10.4% increase over a relatively short period indicates a steady and continuous integration process, reinforcing the suitability of HA as a cranioplasty material. Data on the bone integration rates of porous HA implants

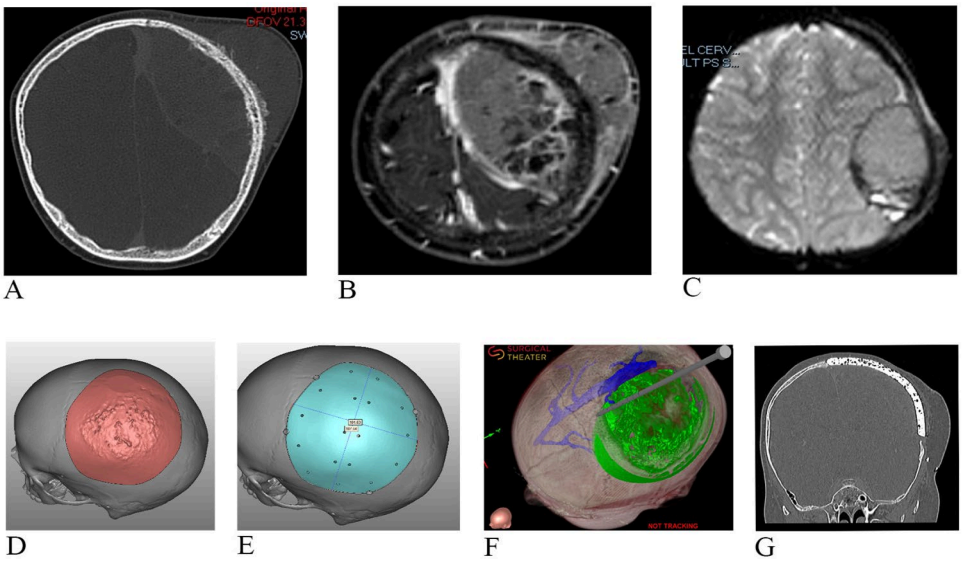

Fig. 3 Implant nº 13, bone metastasis from Ewing sarcoma: **a** Axial CT scan, bone window of a huge transosseous left parietal tumor with evidence of irregular and rarefied bone, and a wide scalp swelling. **b** Axial Gadolinium-enhanced T1 weighted imaging, showing a ring enhancement and an inhomogeneous contrast uptake inside the tumor, due to the presence of intralesional necrotic-cystic areas and calcifications. **c** Axial DWI (diffusion-weighted imaging), showing posterior areas of restricted diffusion, indicative of a high-grade poorly differentiated tumor. **d** 3-D project of the bone resection area. **e** 3D design of the implant with measurement of the orthogonal diameters (107.54 mm × 101.63 mm). The area of the bone defect to be covered by the implant was10531 mm2 and its volume was 52.229 cm3. **f** Augmented reality neuronavigation 3-D image (Surgical Theater ®, Cleveland, OH, USA) of the transosseous and dural infiltration and the surrounding limit of the craniectomy (in **green**) and its relationship with the upper sagittal sinus (in **blue**). "One-step" "en bloc" tumor removal and reconstruction by a bioceramic porous hydroxyapatite custom-made implant was carried out and a rotational pedicled flap, autologous grafting of a muscular cutaneous flap and skin grafts from thigh were used to fill the cutaneous gap with plastic surgeons. **g** Early post-operative CT scan verified the perfect match of the craniectomy margins with the cranioplasty and its satisfying osteointegration

have been published [6, 14, 15, 32, 45, 55], but they refer to a longer observational period, ranging from the first six months to two years after surgical implantation, and they reported a slightly slower pace of osteointegration than we observed. The progression from 72.2% to 82.6% in our surgical series, suggests that bone remodeling and regeneration processes are actively ongoing, with the HA implant gradually integrating into the patient's native bone structure. Additionally, previous preclinical studies on animal models and in vivo have demonstrated that porous HA can support osteointegration and enhance the osteogenic process within the prosthesis [33, 34]. The observed pace of osteointegration is highly encouraging for several reasons. First, the rapid early integration is likely to enhance the mechanical stability of the implant, reducing the risk of complications such as fractures or dislocations during the critical early postoperative period. Second, the continued increase in bone density at 3 months suggests that the implant is not only maintaining its initial integration but is also progressively strengthening its bond with the surrounding bone. This sustained integration likely contributes to the long-term durability of the reconstruction, which is essential for patients recovering from large calvarial tumor resections. The gradual increase in osteointegration also implies that the implant is becoming more mechanically resilient over time, which could explain the absence of implant-related complications, such as fractures, in this study. Our series' osteointegration results could offer insight into a question posed in the literature: 'Should osseointegration be a target during cranioplasty?' In 2016, Stefini and Zanetti [48] commented on this topic: "The healing of the skull and the restoration of its integrity depend on both biological and mechanical requirements". They added that the biological requirements rely on the presence of bone cells capable of supporting healing and an adequate vascular supply, while the mechanical requirements are determined by the degree of rigidity and stability of the "craniolacunia–bone flap" system, which mainly is influenced bt the surgical fixation technique [48].

Furthermore, our data highlight the dynamic nature of the osteointegration process. The early phase, as evidenced by the 6-week CT scan, appears to be characterized by a rapid initial response, possibly driven by the favorable biocompatibility and porosity of HA, which promotes osteoblast migration and new bone formation. Porous HA is osteoconductive and promotes tissue ingrowth and vascularization [29]. Moreover, its porosity facilitates the colonization of osteogenic and nutrient cells, which enhances capillarity [21]. In a review on the state-of-art of materials used in cranioplasty, Siracusa et al. [41] argue that materials promoting vascularization and bone tissue regeneration are preferable to other materials. The subsequent period leading up to the 3-month scan in our sample, reflects a consolidation phase, where the newly formed bone continues to mature and integrate with the HA prosthesis. These findings align with previous smaller studies, reinforcing the notion that HA can effectively enhance the structural integrity of reconstructed calvarial areas [32, 42]. The study also allows critical evaluation of HA as a cranioplasty material in comparison to other commonly used substances, such as titanium, acrylic resins, and plastic polymers. While titanium is a strong material and is biologically inert [49], its poor thermoresistance and limited bone regeneration capability make it less suitable for cranioplasty than other materials with greater biocompatibility such as HA. Malleability, low cost and ease of retrieval, are the principal advantages of acrylic resins and plastic polymers. However, they have limited biocompatibility [3, 34, 38], poor thermostability and potential toxicity to surrounding soft tissues. HA stands out for its enhanced biocompatibility, closely resembling that of natural bone [45]. This similarity not only facilitates better osteointegration but also minimizes the risks of allergic reactions, infections, and implant rejection. The absence of postoperative complications directly related to the HA prostheses further underscores the material's reliability and safety. Moreover, the study's findings on osteointegration are particularly noteworthy. Implants n° 9 to 13, which showed a gap between the prosthesis and the host bone, had significantly lower osteointegration rates compared to other implants in the series. This discrepancy highlights the crucial role of surgical precision in minimizing gaps between the prosthesis and the native bone. The use of piezosurgery and neuronavigation was instrumental in achieving such precision, allowing for a highly accurate matching of resection margins with implant contours. This accuracy is likely a key factor contributing to the favorable osteointegration outcomes observed in this study, as confirmed by early postoperative imaging. The consistency in surgical techniques and the method of osteointegration assessment used across the patient cohort enhances the reliability of our findings and correspond to MRI data related to vascular and fibrous tissue proliferation, even though those were collected for just more than one third of our patients. Additionally, HA's porosity, which allows for the incorporation of bioactive molecules such as antibiotics, is another advantage highlighted in this study. This characteristic likely contributes to the absence of postoperative infection observed in our patients and the low infection rates in published series [19, 24], making HA a structurally sound and effective option comparable to other heterologous materials for repairing cranial defects. In this regard, data gathered from three recent multicenter European studies evaluating the complication rate of patients undergoing porous HA cranioplasty implantation are indeed intriguing [16, 56, 57]. Our study also demonstrates that HA supports new bone growth even in cases where a synthetic dural patch is used, as was the case for the majority of patients in this series, confirming literature data [7]. This finding expands

the potential applications of HA in complex cranial reconstructions, offering a promising solution for patients with extensive calvarial defects. These findings have significant implications for clinical practice. The demonstrated effectiveness of HA in promoting early osteointegration, enhancing mechanical strength, and supporting bone regeneration suggests that it should be considered the preferred material for cranioplasty in patients undergoing calvarial tumor resection. Moreover, the integration of advanced surgical techniques like piezosurgery and neuronavigation has the potential to further optimize surgical outcomes, ensuring precise alignment of implants and reducing the likelihood of complications. However, despite the promising results, the study does have limitations that must be acknowledged. The small sample size and the absence of a control group limit the generalizability of the findings. Additionally, the lack of histological confirmation of osteogenesis and bone regeneration highlights the need for further research. Future studies should aim to include larger patient cohorts and incorporate histological analyses to validate these findings and explore the broader applicability of HA in neurosurgical practice.

Conclusions

This study underscores the significant advantages of using HA for one-step calvarial reconstruction following tumor resection. The material's superior biocompatibility, early onset of osteointegration, and capacity for bioactive molecule incorporation such as antibiotics make it an ideal choice for cranioplasty. While the findings are promising, further research is necessary to confirm these results and establish HA as a standard material for calvarial reconstructions in different patient populations.

Authors' contributions Conceptualization, R.M.; methodology, R.M. and F.S.; validation, F.S.; formal analysis, R.M., M.T.B., M.D., C.D.; investigation, L.S., E.M.N.; data curation, L.S. and L.d.G.; writing—original draft preparation, R.M.; writing—review and editing, F.S. All authors read and approved the final manuscript.

Funding This research received no external funding.

Data availability The study protocol and informed consent are available upon motivated request to the corresponding authors (raffamessina@gmail.com AND/OR raffaella.messina@uniba.it).

Declarations

Ethical approval All procedures performed in studies involving human participants were in accordance with the ethical standards of the institutional and/or national research committee and with the 1964 Helsinki declaration and its later amendments or comparable ethical standards. The Human Investigation Committee (IRB) of University B approved this study.

Consent to participate and consent to publish Informed consent was obtained from all individual participants included in the study.

Competing interests The authors declare no competing interests.

References

1. Alkhaibary A, Alharbi A, Alnefaie N, Oqalaa Almubarak A, Aloraidi A, Khairy S (2020) Cranioplasty: a comprehensive review of the history, materials, surgical aspects, and complications. World Neurosurg 139:445–452
2. Alshareef M, Alshareef A, Vasas T, Shingala A, Cutrone J, Eskandari R (2022) Pediatric cranioplasty using hydroxyapatite cement: a retrospective review and preliminary computational model. Pediatr Neurosurg 57(1):40–49
3. Andrzejak S, Fortuniak J, Wróbel-Wiśniewska G, Zawirski M (2005) Clinical evaluation of the polypropylene-polyester knit used as a cranioplasty material. Acta Neurochir (Wien) 147(9):973–6 (**discussion 976**)
4. Bassi M, Antonelli V, Tomassini A, Maimone G, D'Andrea M, Campobassi A, Gessaroli M, Tosatto L (2021) Synchronized "One-Step" resection and cranio-orbital reconstruction for spheno-orbital lesions with custom made implant. J Craniofac Surg 32(5):1870–1873
5. Binhammer A, Jakubowski J, Antonyshyn O, Binhammer P (2020) Comparative cost- effectiveness of cranioplasty implants. Plast Surg 28:29–39
6. Brie J, Chartier T, Chaput C, Delage C, Pradeau B, Caire F, Boncoeur MP, Moreau JJ (2013) A new custom made bioceramic implant for the repair of large and complex craniofacial bone defects. J Cranio-Maxillofacial Surg 41:403–407
7. Bruno Z, Angelo N, Riccardo S, Nicola Z, Stefano P, Camillo PP, Federico N, Carlotta M (2020) Custom-made hydroxyapatite cranioplasty: radiological and histological evidence of bone-biomaterial osteointegration in five patients. Asian J Neurosurg 15(1):198–203
8. Carolus A, Weihe S, Schmieder K, Brenke C (2017) One-step CAD/CAM titanium cranioplasty after drilling template-assisted resection of intraosseous skull base meningioma: technical note. Acta Neurochir (Wien) 159(3):447–452
9. Castle M, Rivero M, Marquez J (2013) Primary Ewing's sarcoma of the skull: radical resection and immediate cranioplasty after chemotherapy. A technical note Childs Nerv Syst 29(2):303–306
10. Chen TM, Wang HJ (2002) Cranioplasty using allogenic perforated demineralized bone matrix with autogenous bone paste. Ann Pediatr Surg 49(3):272
11. d'Avella E, Somma T, Fabozzi GL, Committeri U, Romano A, Cappabianca P, Cavallo LM (2024) Endoscopic transorbital and transcranial multiportal resection of a sphenoorbital meningiomas with custom bone 3D printing reconstruction: case report. Head Neck 46(2):E18–E25
12 Della Puppa A, Mottaran R, Scienza R (2010) Image-guided cranial osteoma resection and bioceramic porous hydroxyapatite custom-made reconstruction in a one-step surgical procedure. Technical notes and illustrative case. Acta Neurochir (Wien) 152(1):155–9
13 Fahem MM, Das RK, Luther H, Ali AH (2024) Template routed patient-specific implant for 1-stage cranioplasty. Oper Neurosurg (Hagerstown) 27(3):337–346
14. Frassanito P, De Bonis P, Mattogno PP, Mangiola A, Novello M, Brinchi D, Pompucci A, Anile C (2013) The fate of a macroporous hydroxyapatite cranioplasty 4 years after implantation:

macroscopical and microscopical findings in a case of recurrent atypical meningioma. Clin Neurol Neurosurg 115:1496–1498
15. Fricia M, Passanisi M, Salamanna F, Parrilli A, Giavaresi G, Fini M (2015) Osteointegration in custom-made porous hydroxyapatite cranial implants: from reconstructive surgery to regenerative medicine. World Neurosurg 84:591.e511-591.e596
16. Fricia M, Nicolosi F, Ganau M, Cebula H, Todeschi J, Santin MDN, Nannavecchia B, Morselli C, Chibbaro S (2019) Cranioplasty with porous hydroxyapatite custom-made bone flap: results from a multicenter study enrolling 149 patients over 15 years. World Neurosurg 121:160–165
17. Galluzzi P, De Francesco S, Giacalone G, Cerase A, Monti L, Vallone IM, Lazzeretti L, Venturi C, Hadjistilianou T (2011) Contrast-enhanced magnetic resonance imaging of fibrovascular tissue ingrowth within synthetic hydroxyapatite orbital implants in children. Eur J Ophthalmol 21(5):521–528
18. Gerstl JVE, Rendon LF, Burke SM, Doucette J, Mekary RA, Smith TR (2022) Complications and cosmetic outcomes of materials used in cranioplasty following decompressive craniectomy-a systematic review, pairwise meta-analysis, and network meta-analysis. Acta Neurochir (Wien) 164(12):3075–3090
19. Ginebra MP, Traykova T, Planell JA (2006) Calcium phosphate cements as bone drug delivery systems: a review. J Control Release 113(2):102–110
20. Guerrini F, Dallolio V, Grimod G, Cesana C, Vismara D, Franzin AB (2017) It is time to reduce free-hand manipulation: case report of our proposal for an innovative 1-step cranioplasty. World Neurosurg 107:1052.e7-1052.e10
21. Gunzburg R, Szpalski M, Passuti N, Aebi M (2002) The use of bone substitutes in spine surgery: a state-of-the-art review; Springer: Berlin/Heidelberg, Germany, pp 129. ISBN 13:9783540426875
22. Hardy H, Tollard E, Derrey S, Delcampe P, Péron J-M, Fréger P, Proust F (2012) Clinical and ossification outcome of custom-made hydroxyapatite prothese for large skull defect. Neurochirurgie 58(1):25–29
23 Henry J, Amoo M, Taylor J, O'Brien DP (2021) Complications of cranioplasty in relation to material: systematic review, network meta-analysis and meta-regression. Neurosurgery 89(3):383–394
24. Jain AK, Panchagnula R (2000) Skeletal drug delivery systems. Int J Pharm 206(1–2):1–12
25. Kauke-Navarro M, Knoedler L, Knoedler S, Deniz C, Stucki L, Safi AF (2024) Balancing beauty and science: a review of facial implant materials in craniofacial surgery. Front Surg 24(11):1348140
26. Klassen AF, Cano SJ, Scott A, Snell L, Pusic AL (2010) Measuring patient-reported outcomes in facial aesthetic patients: development of the FACE-Q. Facial Plast Surg 26:303–309
27. Klassen AF, Cano SJ, Scott AM, Pusic AL (2014) Measuring outcomes that matter to face-lift patients: development and validation of FACE-Q appearance appraisal scales and adverse effects checklist for the lower face and neck. Plast Reconstr Surg 133(1):21–30
28. Klassen AF, Cano SJ, Schwitzer JA, Scott AM, Pusic AL (2015) FACE-Q scales for health-related quality of life, early life impact, satisfaction with outcomes, and decision to have treatment: development and validation. Plast Reconstr Surg 135(2):375–386
29. Kwarcinski J, Boughton P, Ruys A, Doolan A, Van Gelder J (2017) Cranioplasty and craniofacial reconstruction: a review of implant material, manufacturing method and infection risk. Appl Sci 7:276
30. Liu L, Lu ST, Liu AH, Hou WB, Cao WR, Zhou C, Yin YX, Yuan KS, Liu HJ, Zhang MG, Zhang HJ (2020) Comparison of complications in cranioplasty with various materials: a systematic review and meta-analysis. Br J Neurosurg 34(4):388–396
31. Longmire NM, Wong Riff KWY, O'Hara JL, Aggarwala S, Allen GC, Bulstrode NW, Forrest CR, French BM, Goodacre TEE, Marucci D, Norris JH, Panchapakesan V, Piplani B, Pusic AL, Vercruysse HJ, Klassen AF (2017) Development of a new module of the FACE-Q for children and young adults with diverse conditions associated with visible and/or functional facial differences. Facial Plast Surg 33(5):499–508
32. Maenhoudt W, Hallaert G, Kalala JP, Baert E, Dewaele F, Bauters W, Van Roost D (2018) Hydroxyapatite cranioplasty: a retrospective evaluation of osteointegration in 17 cases. Acta Neurochir (Wien) 160(11):2117–2124
33. Martini L, Staffa G, Giavaresi G, Salamanna F, Parrilli A, Serchi E, Pressato D, Arcangeli E, Fini M (2012) Long-term results following cranial hydroxyapatite prosthesis implantation in a large skull defect model. Plast Reconstr Surg 129:625e–635e
34. Mastrogiacomo M, Scaglione S, Martinetti R, Dolcini L, Beltrame F, Cancedda R, Quarto R (2006) Role of scaffold internal structure on in vivo bone formation in macroporous calcium phosphate bioceramics. Biomaterials 27:3230–3237
35. Meyers A, Krebs J, Xia T, Kshettry VR, Angelov L, Nagel S, Rampazzo A, Gharb BB (2023) Prognosis-guided reconstruction of scalp and skull defects in neurosurgical patients. Ann Plast Surg 91(2):225–231
36. Murphy RJ, Wolfe KC, Liacouras PC, Grant GT, Gordon CR, Armand M (2015) Computer-assisted single-stage cranioplasty. Annu Int Conf IEEE Eng Med Biol Soc 4910–3. https://doi.org/10.1109/EMBC.2015.7319493
37. Oji T, Sakamoto Y, Miwa T, Nakagawa Y, Yoshida K, Kishi K (2016) Usefulness of an osteotomy template for skull tumorectomy and simultaneous skull reconstruction. J Craniofac Surg 27(6):1565–1567
38 Poetker DM, Pytynia KB, Meyer GA, Wackym PA (2004) Complication rate of transtemporal hydroxyapatite cement cranioplasties: a case series review of 76 cranioplasties. Otol Neurotol 25(4):604–9
39. Rubeli SL, D'Alonzo D, Mueller B, Bartlomé N, Fankhauser H, Bucheli E, Conen A, Fandino J, Fux CA (2019) Implementation of an infection prevention bundle is associated with reduced surgical site infections in cranial neurosurgery. Neurosurg Focus 47(2):E3
40. Sahoo NK, Thakral A, Kumar S, Kulkarni V (2024) Flap design for cranial reconstruction: an analysis of craniectomy and cranioplasty incisions. J Maxillofac Oral Surg 23(2):242–247
41 Siracusa V, Maimone G, Antonelli V (2021) State-of-art of standard and innovative materials used in cranioplasty. Polymers (Basel) 13(9):1452
42. Spennato P, Canella V, Aliberti F, Russo C, Ruggiero C, Nataloni A, Lombardo M, Cinalli G (2020) Hydroxyapatite ceramic implants for cranioplasty in children: a retrospective evaluation of clinical outcome and osteointegration. Childs Nerv Syst 36(3):551–558
43 Sprio S, Fricia M, Maddalena GF, Nataloni A, Tampieri A (2016) Osteointegration in cranial bone reconstruction: a goal to achieve. J Appl Biomater Funct Mater 14(4):e470–e476
44 Staffa G, Nataloni A, Compagnone C, Servadei F (2007) Custom made cranioplasty prostheses in porous hydroxy-apatite using 3D design techniques: 7 years experience in 25 patients. Acta Neurochir 149:161–170 (**discussion 170**)
45. Staffa G, Barbanera A, Faiola A, Fricia M, Limoni P, Mottaran R, Zanotti B, Stefini R (2012) Custom made bioceramic implants in complex and large cranial reconstruction: a two-year follow-up. J Craniomaxillofac Surg 40:e65–e70
46 Stefini R, Zanotti B, Nataloni A, Martinetti R, Scafuto M, Colasurdo M, Tampieri A (2015) The efficacy of custom-made porous hydroxyapatite prostheses for cranioplasty: evaluation of post-marketing data on 2697 patients. J Appl Biomater Funct Mater 13(2):e136-44
47. Stefini R, Esposito G, Zanotti B, Iaccarino C, Fontanella MM, Servadei F (2013) Use of "custom made" porous hydroxyapatite

implants for cranioplasty: postoperative analysis of complications in 1549 patients. Surg Neurol Int 4:12
48. Stefini R, Zanetti U (2016) Letter to the editor: should osseointegration be a target to achieve during cranioplasty? J Neurosurg 125(4):1051–1052
49. Stoodley MA, Abbott JR, Simpson DA (1996) Titanium cranioplasty using 3-D computer modelling of skull defects. J Clin Neurosci 3(2):149–55
50 Verbist M, Vandevelde AL, Geusens J, Sun Y, Shaheen E, Willaert R (2024) Reconstruction of craniomaxillofacial bone defects with 3D-printed bioceramic implants: scoping review and clinical case series. J Clin Med 13(10):2805
51. Wang Y, Wang Y, Wang S, Hou S, Yu D, Zhang C, Zhang L, Lin N (2024) Treatment of wound infections linked to neurosurgical implants. Int Wound J 21(4):e14528
52. Winkler PA, Stummer W, Linke R, Krishnan KG, Tatsch K (2000) Influence of cranioplasty on postural blood flow regulation, cerebrovascular reserve capacity, and cerebral glucose metabolism. J Neurosurg 93:53–61
53. Young CC, Hanak BW, Patel AP, Sekhar LN (2018) Rapid Intraoperative in Situ Synthetic Cranioplasty. World Neurosurg 112:161–165
54. Zaccaria L, Tharakan SJ, Altermatt S (2017) Hydroxyapatite ceramic implants for cranioplasty in children: a single-center experience. Childs Nerv Syst 33(2):343–348
55 Zaed I, Cardia A, Stefini R (2022) From reparative surgery to regenerative surgery: state of the art of porous hydroxyapatite in cranioplasty. Int J Mol Sci 23(10):5434
56 Zaed I, Rossini Z, Faedo F, Fontanella MM, Cardia A, Servadei F (2022) Long-term follow-up of custom-made porous hydroxyapatite cranioplasty in adult patients: a multicenter. European study. Can we trust self-reported complications? J Neurosurg Sci 66(4):335–341
57. Zaed I, Safa A, Spennato P, Mottolese C, Chibbaro S, Cannizzaro D, Faggin R, Frassanito P, Maduri R, Messerer M, Servadei F (2022) A multicentric European clinical study on custom-made porous hydroxyapatite cranioplasty in a pediatric population. Front Surg 23(9):848620